Chinese Journal of Analytical Chemistry 53.3 (2025) 100498

Contents lists available at ScienceDirect

Chinese Journal of Analytical Chemistry

journal homepage: www.elsevier.com/locate/cjac

Molecular docking, dynamic molecular simulation and in silico ADMET screening study of novel bidentate tetrazolyl-adipate anti-HIV drugs candidate

Fatimazohra LENDA[a,*], Mohammed ER-RAJY[b], Asmae El CADI[a], Hamada IMTARA[c,*], Farhate GUENOUN[d], Hassan ALLOUCHI[e], Somdutt MUJWAR[f], Khalid NAJOUI[g], Omar M. NOMAN[h], Jean MARTINEZ[i], Frédéric LAMATY[i], Menana ELHALLAOUI[b]

[a] Department of Chemistry, Faculty of Sciences, Physical-Chemical Laboratory of Materials, Natural Substances and the Environment (LAMSE), Techniques of Tangier-University Abdelmalek Essaadi, Tangier, Morocco
[b] LIMAS Laboratory, Faculty of Sciences Dhar El Mahraz, Sidi Mohamed Ben Abdellah University, Fez, Morocco
[c] Faculty of Medicine, Arab AmericanUniversity Palestine, Jenin 44862, Palestine
[d] Laboratory of Chemistry-Biology Applied to the Environment, Moulay Ismail University Faculty of Sciences, Meknes, Morocco
[e] Laboratory of Physical-Chemical, SIMBA EA 7502, Faculty of Pharmacy, University of Tours, 37200 Tours, France
[f] Chitkara Colleges of Pharmacy, Chitkara University, Rajpura, Punjab 140401, India
[g] CRMEF TTH, BP 3117, Souani, Avenue My Abdelaziz, Tangier, Morocco
[h] Department of Pharmacognosy, College of Pharmacy, King Saud University, Riyadh 11451, Saudi Arabia
[i] IBMM, University of Montpellier, CNRS, ENSCM, 34095 Montpellier, France

ARTICLE INFO

Keywords:
Bidentate tetrazolyl adipic ester
CYP3A4
Anti-HIV
Molecular docking
MDS

ABSTRACT

In order to develop specific inhibitors of CYP3A4, we chose new derivatives of adipic acid the 2,5-(5-aryl tetrazol-2yl) dimethyl adipate L_1-L_5. During this study, the Ritonavir molecule known as inhibitor of the cytochrome CYP3A4 are chosen as a reference. A molecular docking simulation on the enzyme 7UAZ is conducted for the ligands L_1-L_5, in order to study the predictive binding affinity and the interaction mechanism of the 5-aryltetrazolyl substituents introduced at positions 2 and 5 of adipic acid. A molecular docking study revealed that the relative activation energy level ranged from –10.1 to –7.6 kcal/mol, falling within the range of Ritonavir at –9.0 kcal/mol, which confirms the stability of the ligands within the studied enzyme. The results show that the binding mode of the ligands on the enzyme 7UAZ varies significantly depending on the substituent at the -C5 position of the tetrazole, with the best results obtained for the ligands L_2 and L_5. Then a comparative study based on silico ADMET properties selected only L_2 as a potential inhibitor of CYP3A4. A 100 ns molecular dynamics simulation on the ligand-protein complex highlights the stability of ligand L_2 within the 7UAZ protein.

1. Introduction

In accordance with the tetrazole ring is isosteric from the carboxylic acid action. Moreover, the heterocycle is regarded as particularly important in a variety of disciplines, including pharmacology, biochemistry, and enzymology. Also, substituted tetrazoles have a variety of biologically distinctive properties [1–8]. The key to developing new treatments for chronic and infectious immune diseases is the development of new biomolecules with encouraging pharmacological properties and promising synthesis. In medicinal chemistry, tetrazolic compounds are used in the manufacture of medicines. Cefamandole is an antibiotic, while olmesartan, losartan, and candesartan are antihypertensives that act on angiotensin II inhibition. Also, cenobamate (ontozry) is an antiepileptic (Fig. 1) [9–11]. They also, treat acquiredImmune deficiency syndrome (AIDS) [12] and cancer [13]. Studies have shown that further nitrogen-based compounds have the ability to non-covalently bind to specific receptors and demonstrated their effectiveness in antiviral treatments [14].

Ritonavir (Fig. 2), the reference compound used in this study, has been identified in the literature as an inhibitor of the CYP3A4 enzyme [15,16]. This enzyme is definitively deactivated by ritonavir through a process that remains uncertain [17].

CYP3A4, the primary human enzyme in this work, belongs to the cytochrome P450 superfamily. It is responsible for the biosynthesis and

* Corresponding authors.
E-mail addresses: f.lenda@uae.ac.ma (F. LENDA), hamada.imtara@aaup.edu (H. IMTARA).

https://doi.org/10.1016/j.cjac.2025.100498
Received 27 November 2024; Received in revised form 2 January 2025; Accepted 19 January 2025
Available online 20 January 2025
1872-2040/© 2025 The Authors. Published by Elsevier Ltd on behalf of Changchun Institute of Applied Chemistry Chinese Academy of Sciences. This is an open access article under the CC BY-NC-ND license (http://creativecommons.org/licenses/by-nc-nd/4.0/)

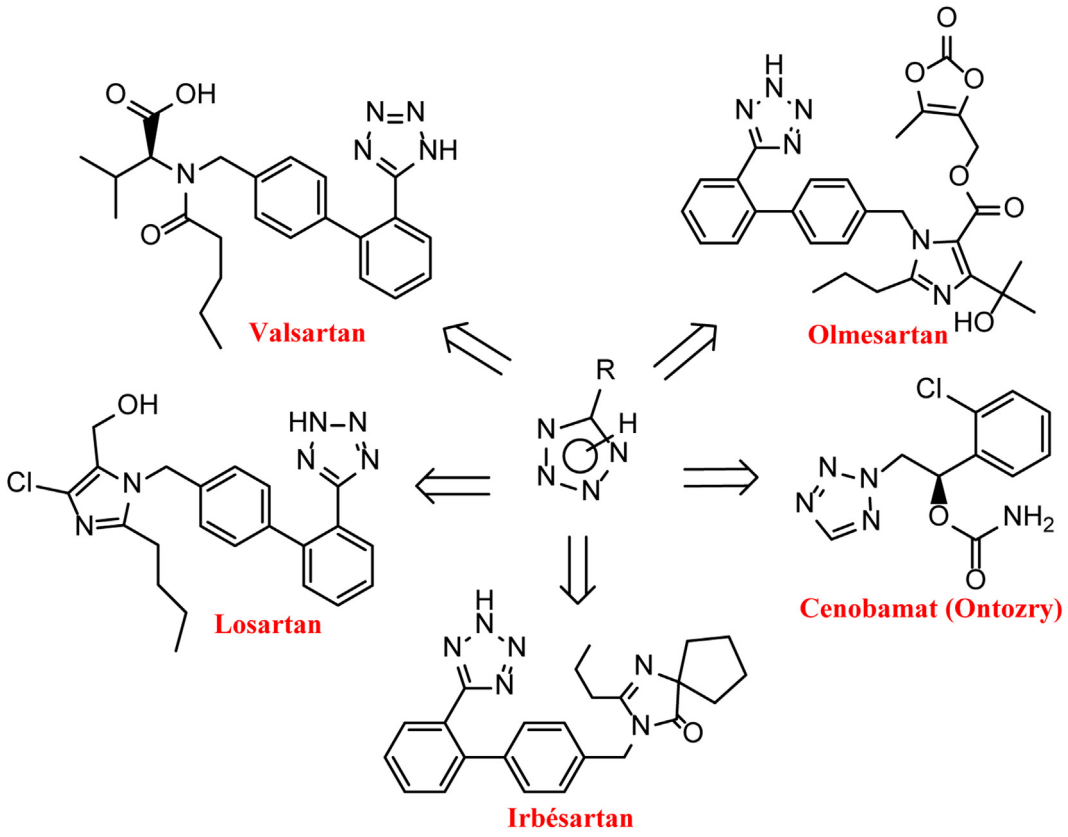

Fig. 1. Illustrations of drugs containing the tetrazole ring.

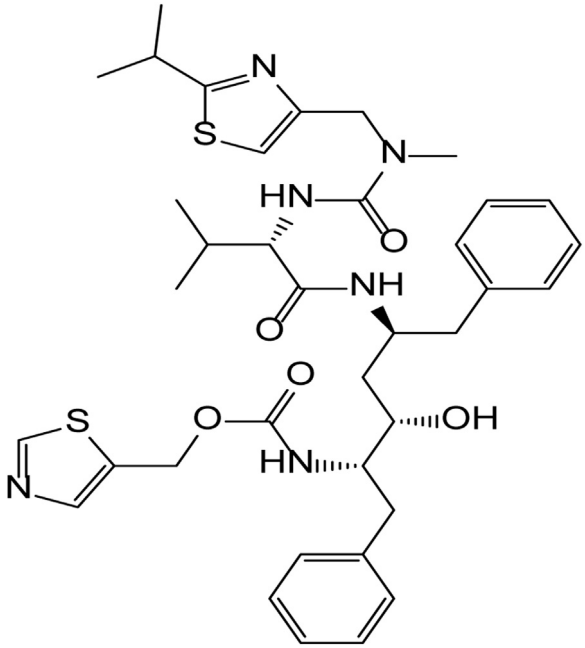

Fig. 2. 2D structure of Ritonavir.

metabolism of xenobiotics [18]. It is essential to monitor one's activity in order to assess the metabolism of medications and identify potentially harmful drug interactions. In addition, the functions as an antiretroviral (anti-HIV) agent by inhibiting the aspartyl protease of the human immunodeficiency virus [19]. Human immunodeficiency virus (HIV) protease inhibitors render the enzyme unable to synthesize the polyprotein precursor Gag-pol, resulting in the production of HIV particles that are morphologically immature and incapable of initiating new infectious cycles. However, in addition to its very low inhibitory activity on human aspartic proteases, the adverse effects of Ritonavir make it necessary to develop new CYP3A4 inhibitors with improved pharmacochemical properties. Combining C5-aryltetrazole with an adipic acid (AA) analogue is an interesting approach to creating hybrid molecules with considerable pharmacological effects.

In this study, we used starting precursors such as methyl meso-2,5-dibromodimethyladipate and 5-aryltetrazole to form the bidentate 2,5-bis (5-aryl tetrazol-2-yl)-dimethyl adipate. In addition, computational studies and molecular docking calculations have also been performed to verify the action potential of these molecules on selected receptor, 7UAZ. Subsequently, these products were subjected to specific ADME-Tox criteria to evaluate their potential pharmacodynamic (PD) and pharmacokinetic (PK) efficiency. In the final phase of this study, a molecular dynamics simulation is conducted to analyze the stability of the complexes obtained during molecular docking.

Furthermore, throughout this research, we discovered the significance of the aromatic side group C5-phenyltetrazolyl, which is comparable to Phe2 from Ritonavir, in the formation of hydrophobic contacts between the ligands under investigation and the amino acid residues from CYP3A4. As shown in Table 1, the L_1-L_5 structures have been proposed as alternatives to Ritonavir.

To select new bidentate tetrazolyl-adipate candidates for anti-HIV drugs, major pharmaceutical companies are increasingly focusing on innovation by adopting new research methodologies and advancing the development of novel compounds. Molecular modeling studies, such as molecular docking, molecular dynamics, and ADMET analysis, are essential tools for identifying and predicting the efficacy of these new drug candidates [20,21].

Table 1
Chemical structure 2D of bidentate 2, 5-bis (5-aryl tetrazol-2yl)-dimethyl adipate L_1–L_5.

	L_1	L_2	L_3	L_4	L_5
Chemical structure	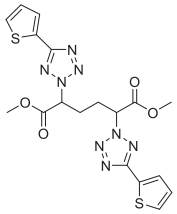	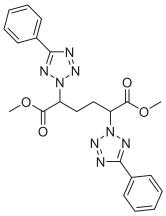	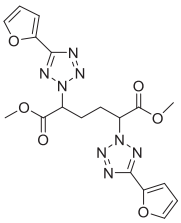	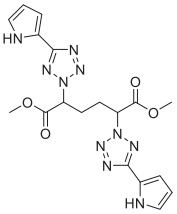	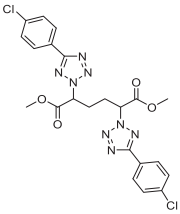

2. Material and methods

2.1. Molecules studied

The synthesis of bidentate 2, 5-bis (5-aryl tetrazol-2yl)-dimethyl adipate, L_1-L_5 series was carried out by reaction of 5-aryltetrazole with methyl meso-2, 5-dibromodimethyladipate 1, which was obtained from adipic acid. The 5-aryletetrazole groups were introduced by successive substitutions of the two bromine atoms and purified firstly by recrystallization from a CH_2Cl_2/hexane mixture and then a second recrystallization from a diethyl ether/ethyl acetate mixture [22]. These different molecules have already been synthesized in previous work [21].

2.2. Molecular docking and molecular dynamic studies

The materials of this search were conducted using the software AutoDockTools-1.5.7, Chem3D Pro 12.0, ChemDraw Ultra 12.0. During this work, we also used Biovia Discovery Studio 2016 client to interpret the results, in order to visualize the existing interactions between the different ligands and the proteins studied. In addition, we revealed the pharmacokinetic properties and toxicity of the ligands using PreADMET [23].

Molecular docking is a highly reliable method that aims to predict the likely interactions between ligands (inhibitor) and the amino acids that make up the receptor (enzyme) in order to minimize the time required for in silico drug discovery [24]. The 3D structure of the 7UAZ protein was obtained by downloading it in PDB format from the PDB database. Anchoring of the L_1-L_5 compounds in the active site of the 7UAZ protein was carried out using Auto Dock Vina according to the standard protocol [25,26]. The ChemOffice drawing tool (ChemDraw 16.0) is first used in an appropriate 2D orientation to determine the L_1-L_5 structures, then using Chem3D 16.0 we adopted the structure with minimized energy [27].

The structures of the various ligands L_1 to L_5 were optimized by the SYBYL-X2.0 software, then introduced into Auto Dock Vina to carry out the simulation by molecular docking [28–30]. The crystal structure of the receptor of Escherichia coli BL21E (PDB ID: 7UAZ), was downloaded from the Protein Data Bank (PDB).

Next, the protein was prepared according to the standard protocol by first removing the crystallized ligand, then the selected water molecules and the cofactors. The grid box was constructed using 40, 40, and 40, oriented in *x*, *y*, and *z* directions, with a grid point spacing of 0.375 Å. The center grid box for 7UAZ (–19.168 Å, –23.904 Å and –14.616 Å). During the modeling process with Auto Dock Vina, the docking algorithm provided a maximum of nine conformers for each ligand considered. Subsequently, through Discovery Studio and PyMOL software, we analyzed and visualized the interactions between the ligands and the target receptor. Finally, molecular dynamic (MD) simulation of the 7UAZ-Ligand complex was performed for 100 ns with the Desmond module of the Schrödinger programmer to assess the binding stability and orientation patterns of the acquired leads from virtual screening [20,23,31].

2.3. Prediction of ADMET properties and in-silico drug-likeness predictions

An additional study of the prediction of compounds L_1 to L_5 by the ADMET method of absorption, distribution, metabolism, excretion, and toxicity was prepared using the Swiss ADMETweb server [32]. The skin permeability value *Kp* indicates information on the cutaneous absorption of the molecules. In silico, *Kp* values for all compounds were within the Ritonavir dosage range of –9.09 cm/s, indicating a low skin permeability range from –5.69 to –7.70 cm/s. Similarly, the distribution and absorption of drug molecules is indicated by the blood-brain barrier (BBB) and gastrointestinal (GI) permeation [33,34].

To defend this study and reinforce the results obtained by molecular docking, we opted to evaluate and compare certain pharmacokinetic and physicochemical properties that dominate the ADMET criteria of compounds L_1 to L_5 and Ritonavir. Several studies suggest that a particular organic molecule can be orally active and is part of drug design if it has high activity towards the chosen target and check the ADMET properties and meet the five rules of Lipinski's [35]. Hydrogen bond acceptors (NHAs) should be less than 10, molecular weight should be less than 500 Da, hydrogen bond donors (NHDs) should be less than 5, total polar surface area (TPSA) should not be more than 140 Å, and log P should not be less than 5 [36].

3. Results and discussion

3.1. Molecular docking studies

Analysis of the results obtained by molecular docking showed that L_1-L_5 bidentate ligands of 2,5-dimethyl-bis (5-(aryl-2-yl)-2H-tetrazol-2-yl) hexanedioate have binding affinities 7UAZ in energy values ranging from –8.1 to –10.1 kcal/mol whereas the binding affinity of ritonavir on the same receptor was –9.0 kcal/mol (Table 2 and Fig. 3).

Compound L_4 formed five hydrogen bond interactions with Cys-442, Arg-105, Ile-443, Gly-444, and Pro-434 of the protein. Compounds L_3 and L_5 showed four hydrogen bond interactions with the active site amino acids Arg-105, Cys-442, Gly- 444, Ala-305, and Arg-105, Cys-442, Gly-444, and Ser-119. Compounds L_1 and L_2 showed three hydrogen bond interactions with Arg-105, Gly-444, Phe-435 and Arg-105, Ile-443, and Gly-444 of the protein, respectively. Ritonavir showed four hydrogen bond interactions with Arg-105, Ser-119, Arg-375, and Ile-443. Hydrophobic interactions were observed for compound L_5 with Ala-305, Ala-448, Ile-369, Ile-443, Cys-442, Phe-447, Val-313, and Met-452. Compound L_2 showed interactions with Ile-369, Ile-443, Gly-444, Cys-442, Phe-435, Ala-305, and Ala-370; compound L_1 with Ala-305, Gly-444, Phe-435, Ile-369 and Cys-442, and compound L_3 with Phe-435, Ala 370, Val-313, Leu-364, and Ile-369. Compound L_4 showed interactions with Ile-301, Ile-369, Phe-435, and Ala-305.

These results suggested that L_2 and L_5 might be better inhibitors of the human enzyme CYP3A4 than L_1, L_3 and L_4, because they showed more significant molecular interactions in addition to a better binding energy of –9.9 and –10.1 kcal/mol in comparison to Ritonavir's –9.0 kcal/mol.

Table 2
Binding affinity and residual amino acid interactions of Compounds L_1-L_5 and Ritonavir with the 7UAZ receptor.

Compounds	Affinity (kcal/mol)	Hydrogen-Bonds	Residual Amino Acid Interactions Hydrophobic/Pi-Anion/ Pi-Cation/Pi-Alkyl/Pi-Sulfur /Other interactions	Van-der Walls Interactions
L_1	–8.3	Arg-105, Gly-444, Phe-435	Ala-305, Gly-444, Phe-435, Ile-369, Cys-442	Ile-443
L_2	–10.1	Arg-105, Ile-443, Gly-444	Ile-369, Ile-443, Gly-444, Cys-442, Phe-435, Ala-305, Ala-370	Ser-119
L_3	–8.8	Arg-105, Cys-442, Gly- 444, Ala-305	Phe-435, Ala-370, Val-313, Leu-364, Ile-369	Ser-119, Ile-118, Ile-443,
L_4	–8.1	Arg-105, Cys-442, Ile-443, Gly-444, Pro-434	Ile-301, Ile-369, Phe-435, Ala-305	Arg-375, Ser-119
L_5	–9.9	Arg-105, Cys-442, Gly-444, Ser-119	Ala-305, Ala-448, Ile-369, Ile-443, Cys-442, Phe-447, Val-313, Met-452	Arg-440, Ile-118
Ritonavir	–9.9	Arg-105, Ser-119, Arg-375, Ile-443	Ile-369, Leu-373, Leu-482, Cys-442, Phe-435	Arg-440, Ile-118

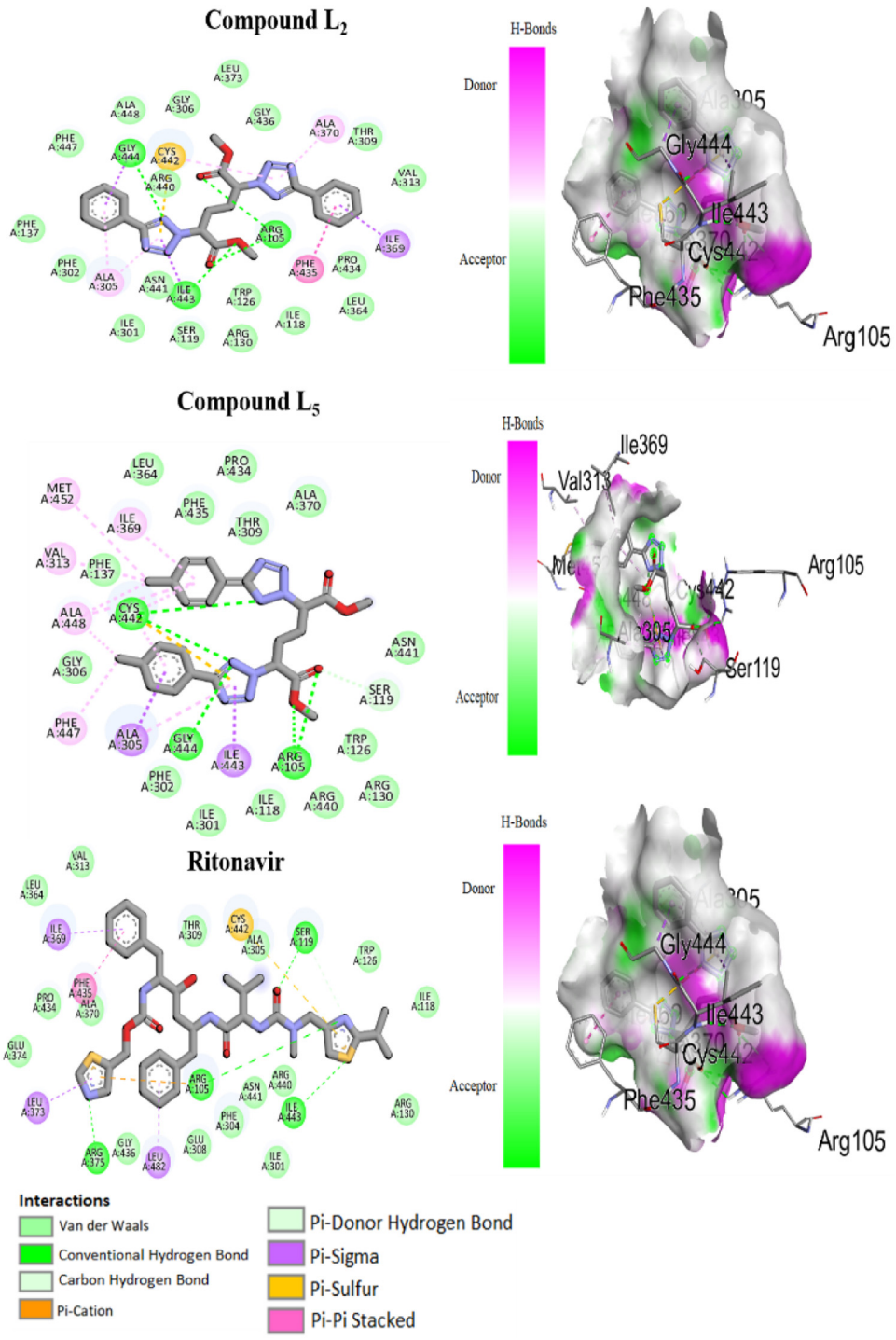

Fig. 3. Binding mode of Compounds L_2, L_5 and Ritonavir with the 7UAZ Receptor 2D (left) and 3D (right) views of the interaction of L_2, L_5 and Ritonavir with the 7UAZ proteins.

Table 3
Drug-likeness predictions of compounds L_1–L_5, computed by SwissADME.

S. N_O	Mol. Wt. (g /mol)	NRB	NHD	TPSA (Å^2)	LogP (cLogP)	Lipinski
L_1	474.52	11	0	196.28	2.58	Yes
L_2	462.46	11	0	139.80	2.57	Yes
L_3	442.39	11	0	166.08	1.28	Yes
L_4	440.42	11	2	171.38	0.94	Yes
L_5	531.35	11	0	139.80	3.64	No

Table 4
Drug-likeness predictions of compounds L_1 to L_5, computed by SwissADME.

Compounds	Skin Permeation Value (log *Kp*) cm/s	GI Absorption	BBB Permeability	Inhibitor Interaction (SwissADME)					
				P-gp Substrate	CYP1A2 Inhibitor	CYP2C19 Inhibitor	CYP2C9 Inhibitor	CYP2D6 Inhibitor	CYP3A4 Inhibitor
L_1	–6.64	Low	No	No	Yes	No	No	No	Yes
L_2	–6.16	High	No	No	Yes	Yes	Yes	No	Yes
L_3	–7.32	Low	No	No	Yes	No	No	No	Yes
L_4	–7.70	Low	No	Yes	Yes	No	No	No	Yes
L_5	–5.69	Low	No	No	Yes	Yes	Yes	No	Yes

GI (Gastro-Intestinal); BBB (Blood Bain Barrier); P-gp (P-GlycoProtein); CYP (Cytochrome-P).

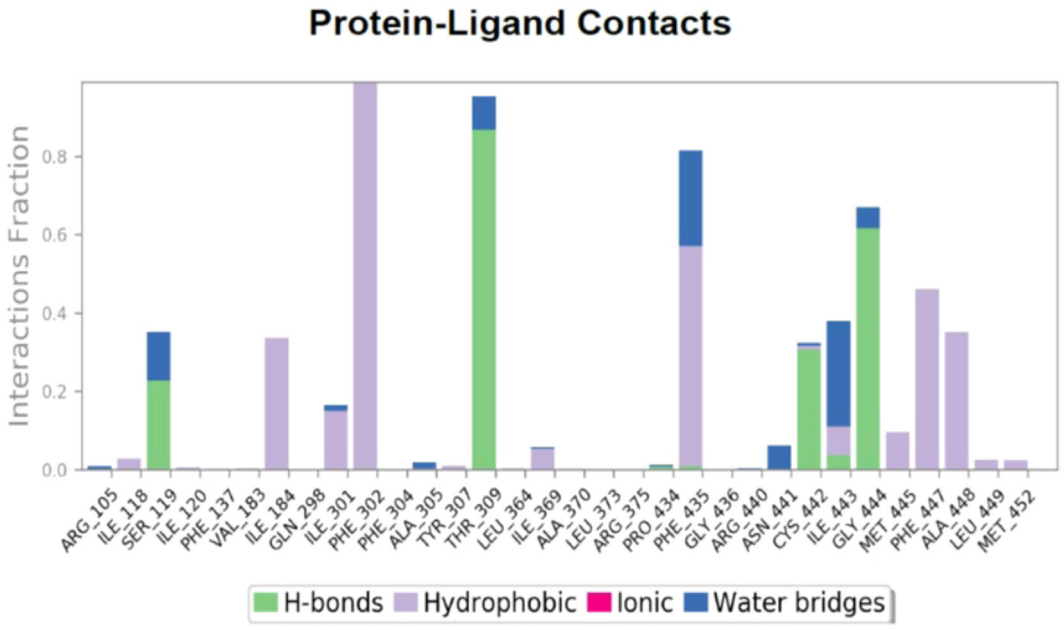

Fig. 4. Interactions observed between the protein ligand complexes during the 100 ns MD simulation.

3.2. Prediction of ADMET properties

Table 3 groups together the various results of in silico prediction of the ADME of compounds L_1 to L_5. Also, the tetrazole bidentate derivative L_2 exhibits high gastrointestinal (GI) absorption. Moreover, several cytochromes, including CYP1A2, CYP2C19, CYP2C9, and CYP3A4, are necessary for the biotransformation of drug metabolism. The Swiss web in silico ADME prediction indicates that the substances from L_2 and L_5 inhibit these cytochromes.

According to the results obtained in Table 3, the SwissADME prediction study revealed that compounds L_1 to L_5 obey Lipinski's five rules and can be orally active, with the exception of compound L_5.

3.2.1. In-silico drug-likeness predictions

The probability of a compound being considered a drug candidate is high and proportional to the value of its score. All the results collected are grouped together in Tables 3 and 4.

The ADME prediction results for the five compounds, including, skin permeation value, gastrointestinal absorption, BBB permeability, P-glycoprotein substrate, inhibition capacity, and cytochrome P450 enzyme substrate, obtained from the Swiss ADME prediction are listed in Table 4. Then, the SwissADME prediction website was used to calculate the ADME properties.

From Table 4, it can be observed that strong gastrointestinal absorption is exhibited only by the L_2 molecule among the five compounds. Furthermore, none of the selected molecules are capable of crossing the BBB. Compound L_4 was identified as a substrate of glycoproteins, and the four tested compounds were unable to inhibit the cytochrome P450 enzyme subtype 1A2. However, all the compounds inhibited the cytochrome P450 enzyme subtype 2D6, while all five tested compounds were inhibitors of the cytochrome P450 enzyme subtype 3A4. In conclusion, compound L_2, which conforms to the golden triangle rule, appears to have a more favorable ADMET profile.

3.3. Molecular docking simulation

Interpretation of the molecular docking results of this study revealed an acceptable type of binding, but protein flexibility and solvent influ-

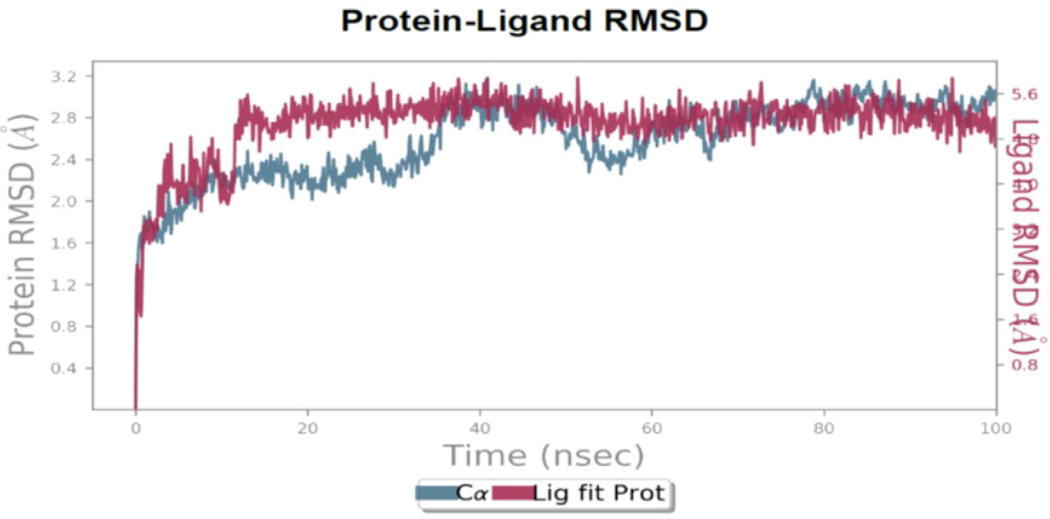

Fig. 5. The RMSD visualized during the MD simulation of 100 ns to 7UAZ-L_2 complexed target.

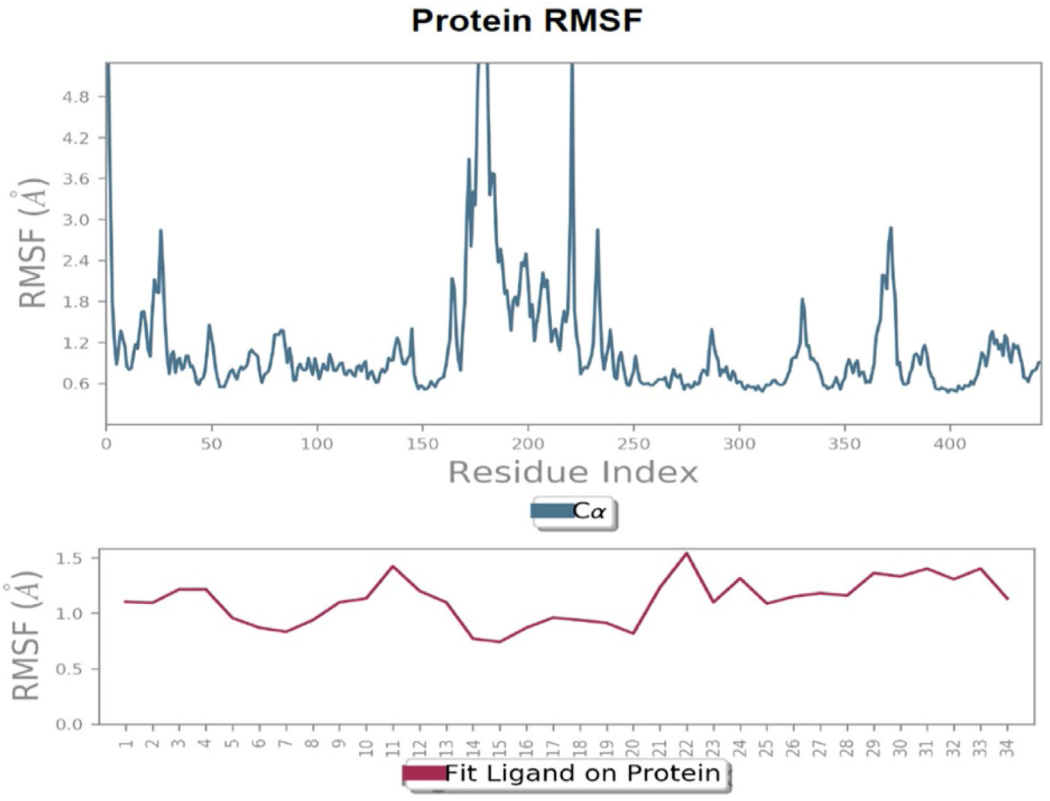

Fig. 6. The tracing of the protein RMSF and the fit ligand L_2 on the protein 7UAZ by a simulation at 100 ns.

ence were not fully considered. To support the results revealed during this study of the therapeutic potential of the ligand L_2 with the target protein, we further evaluated the conformational stability of this protein and the ligand-receptor complex docked as well as the established interactions (Fig. 4). The results of molecular docking between the ligand L_2 and 7UAZ receptor were validated via a 100 ns molecular dynamics simulation (MDS). This method is based on the protocol established in the studies [37]. The stability of the conformations formed of the protein ligand complex, as well as the interactions and fluctuations produced during the MD trajectories, have been verified by the calculation of the mean square deviation parameters (RMSD) and of the mean square fluctuations (RMSF) in Figs. 5 and 6. Its two methods use an adapted force field over a 100 ns time scale with the Schrodinger software package.

The alpha-carbon values for the protein-ligand complex have remained stable since the start of the simulation at 10 ns and from 35 ns to 100 ns. During the period 10–35 ns, it underwent minimal conformational movement in the tolerable range of 3 Å. Overall, the ligand L_2 is stable in the cavity and does not separate from the protein despite some fluctuations in the permitted range. The analysis of the bonds established by the ligand L_2 with the target protein during 100 ns of the MD simulation evolution to record the formation of a stable macromolecular complex via the elaboration of hydrogen bonds with Ser-119, Thr-309, Pro-434, Phe-435, Cys-442, Ile-443, and Gly-444, water bridges with

Arg-105, Ala-305, Arg-440, Asn-441, Cys-442, and Ile-443, and the hydrophobic interactions Ile-184 and 301, Phe-302, 435 and 447, Met-445, and Ala-448 (Fig. 4). The RMSF values of the protein and the fit ligand L_2 with the protein 7UAZ were also recorded in the tolerable range of 0.8–1.6 Å. showed less fluctuations in the range of 0.6–2.8 Å, with the exception of a few index residues between 180 and 225. In conclusion, the ligand L_2 has the capacity to form a stable complex with the protein 7UAZ throughout the simulation (Fig. 5).

In conclusion, L_1-L_5 structures have been proposed as less complex and less expensive alternatives to Ritonavir. Furthermore, L_2 exhibits a greater affinity for the CYP3A4 enzyme, making it a potential model for the search for more effective inhibitors for this enzyme.

4. Conclusion

In this study, a series of tetrazole bidentates are proposed as CYP3A4 enzyme inhibitors. The functional and structural data of compounds L_1 to L_5 explain the significant interactions with enzymes. Furthermore, the resulting interactions of the phenyls (Ph1 and Ph2) of the ligand (L_2) dimethyl hexanedioate 2, 5-bis (5-phenyltetrazol-2yl) with the enzyme are fully compatible with the interactions detected of Ritonavir with the same enzyme. In particular, donor/acceptor groups, H-bonds, and the aromaticity of the Phe2 side group play a major role in the formation of hydrophobic interactions. The results of the study also showed that the binding capacity and affinity of the L_2 and L_5 ligands are better for Ritonavir; these compounds are highly flexible and capable of adopting an optimized conformation that induces significant key interactions between the ligands and the enzyme. This underlines the influence of polar interactions in CYP3A4-ligand assembly. More importantly, two of the compounds, L_2 and L_5, have better affinity for the CYP3A4 enzyme, are smaller than Ritonavir, and could therefore provide a new model for a second-generation inhibitor to further optimize the pharmacophore model. In addition, the bidentate diester L_2, whose phenyl rings are associated with two tetrazoles, satisfies both Lipinski's and Pfizer's rules. In conclusion, compound L_2 conforming to the golden triangle rule may have a more favorable ADMET profile. A further study is carried out using molecular dynamics simulation at 100 ns. Calculation of the RMSD and RMSF parameters demonstrated the stability of the L_2-7UAZ complex. The L_2 ligand exhibits stable behavior inside the 7UAZ protein cavity and does not leave it during the 100 ns. According to the various studies carried out in this project, the selected L_2 molecule could be used as a new model of CYP3A4 cytochrome inhibitor.

Declarations, ethical approval and participation consent

Not applicable.

Consent for publication

All authors have consented to the publication of this work.

Funding information

Researchers supporting project RSPD2025R1087, King Saud University, Riyadh, Saudi Arabia.

Data availability

The data and materials supporting the findings of this study are included in the published article.

Declaration of competing interest

The authors declare that they have no competing interests.

CRediT authorship contribution statement

Fatimazohra LENDA: Writing – original draft, Software, Formal analysis, Data curation, Conceptualization. **Mohammed ER-RAJY:** Methodology, Investigation, Funding acquisition, Formal analysis, Conceptualization. **Asmae El CADI:** Data curation, Formal analysis, Writing – review & editing. **Hamada IMTARA:** Methodology, Investigation, Funding acquisition, Formal analysis, Conceptualization. **Farhate GUENOUN:** Writing – review & editing, Formal analysis, Data curation. **Hassan ALLOUCHI:** Writing – review & editing, Formal analysis, Data curation. **Somdutt MUJWAR:** Writing – review & editing, Formal analysis, Data curation. **Khalid NAJOUI:** Project administration, Methodology, Investigation. **Omar M. NOMAN:** Writing – review & editing, Visualization, Validation, Methodology, Funding acquisition. **Jean MARTINEZ:** Project administration, Methodology, Investigation. **Frédéric LAMATY:** Writing – review & editing, Visualization, Validation, Methodology, Funding acquisition. **Menana ELHALLAOUI:** Project administration, Methodology, Investigation.

Acknowledgment

The authors extend their appreciation to the researchers supporting project number (RSPD2025R1087), King Saud University, Riyadh, Saudi Arabia.

References

[1] Romagnoli R, Baraldi PG, Salvador MK, Preti D, Aghazadeh Tabrizi M, Brancale A, Fu XH, Li J, Zhang SZ, Hamel E, Bortolozzi R, Basso G, Viola G. Synthesis and evaluation of 1,5-disubstituted tetrazoles as rigid analogues of combretastatin A-4 with potent antiproliferative and antitumor activity. J Med Chem 2012;55:475–88. doi:10.1021/jm2013979.

[2] Yella R, Khatun N, Rout SK, Patel BK. Tandem regioselective synthesis of tetrazoles and related heterocycles using iodine. Org Biomol Chem 2011;9:3235–45. doi:10.1039/C0OB01007C.

[3] Herr RJ. 5-Substituted-1*H*-tetrazoles as carboxylic acid isosteres: medicinal chemistry and synthetic methods. Bioorg Med Chem 2002;10:3379–93. doi:10.1016/S0968-0896(02)00239-0.

[4] Jursic BS, Leblanc BW. Preparation of tetrazoles from organic nitriles and sodium azide in micellar media. J Heterocycl Chem 1998;35:405–8. doi:10.1002/jhet.5570350224.

[5] Monn JA, Valli MJ, True RA, Schoepp DD, Leander JD, Lodge D. Synthesis and pharmacological characterization of l-*trans*-4-tetrazolylproline (ly300020): A novel systemically-active ampa receptor agonist. Bioorg Med Chem Lett 1993;3:95–8. doi:10.1016/S0960-894X(00)80099-2.

[6] Chang CS, Lin YT, Shih SR, Lee CC, Lee YC, Tai CL, Tseng SN, Chern JH. Design, synthesis, and antipicornavirus activity of 1-[5-(4-arylphenoxy)alkyl]-3-pyridin-4-ylimidazolidin-2-one derivatives. J Med Chem 2005;48:3522–35. doi:10.1021/jm050033v.

[7] Katritzky AR, Cai C, Meher NK. Efficient synthesis of 1,5-disubstituted tetrazoles. Synthesis 2007;72:1204–8. doi:10.1055/s-2007-966001.

[8] Singh H, Chawla AS, Kapoor VK, Paul D, Malhotra RK. Medicinal chemistry of tetrazoles. Prog Med Chem 1980;17:151–83. doi:10.1016/s0079-6468(08)70159-0.

[9] Eykyn S, Jenkins C, King A, Phillips I. Antibacterial activity of cefamandole, a new cephalosporin antibiotic, compared with that of cephaloridine, cephalothin, and cephalexin. Antimicrob Agents Chemother 1973;3:657–61. doi:10.1128/AAC.3.6.657.

[10] Wang L, Zhao JW, Liu B, Shi D, Zui Z, Shi XY. Antihypertensive effects of olmesartan compared with other angiotensin receptor blockers: A meta-analysis. Am J Cardiovasc Drugs Drugs Devices Other Interv 2012;12:335–44. doi:10.1007/BF03261842.

[11] Barbieri MA, Perucca E, Spina E, Rota P, Franco V. Cenobamate: A review of its pharmacological properties, clinical efficacy and tolerability profile in the treatment of epilepsy. CNS Neurol Disord Drug Targets 2023;22:394–403. doi:10.2174/1871527321666220113110044.

[12] Yeung KS, Qiu Z, Yang Z, Zadjura L, D'Arienzo CJ, Browning MR, Hansel S, Huang XS, Eggers BJ, Riccardi K, Lin PF, Meanwell NA, Kadow JF. Inhibitors of HIV-1 attachment. Part 9: Aan assessment of oral prodrug approaches to improve the plasma exposure of a tetrazole-containing derivative. Bioorg Med Chem Lett 2013;23:209–12. doi:10.1016/j.bmcl.2012.10.125.

[13] Dhiman N, Kaur K, Jaitak V. Tetrazoles as anticancer agents: A review on synthetic strategies, mechanism of action and SAR studies. Bioorg Med Chem 2020;28:115599. doi:10.1016/j.bmc.2020.115599.

[14] Mikolaichuk OV, Zarubaev VV, Muryleva AA, Esaulkova YL, Spasibenko DV, Batyrenko AA, Kornyakov IV, Trifonov RE. Synthesis, structure, and antiviral properties of novel 2-adamantyl-5-aryl-2H-tetrazoles. Chem Heterocycl Compd 2021;57:442–7. doi:10.1007/s10593-021-02931-5.

[15] Granfors MT, Wang JS, Kajosaari LI, Laitila J, Neuvonen PJ, Backman JT. Differential inhibition of cytochrome P450 3A4, 3A5 and 3A7 by five human immunodeficiency

virus (HIV) protease inhibitors *in vitro*. Basic Clin Pharmacol Toxicol 2006;98:79–85. doi:10.1111/j.1742-7843.2006.pto_249.x.

[16] Mannu J, Jenardhanan P, Mathur PP. A computational study of CYP3A4 mediated drug interaction profiles for anti-HIV drugs. J Mol Model 2011;17:1847–54. doi:10.1007/s00894-010-0890-6.

[17] Loos NHC, Beijnen JH, Schinkel AH. The mechanism-based inactivation of CYP3A4 by ritonavir: What mechanism? Int J Mol Sci 2022;23:9866. doi:10.3390/ijms23179866.

[18] Kumar GN, Rodrigues AD, Buko AM, Denissen JF. Cytochrome P450-mediated metabolism of the HIV-1 protease inhibitor ritonavir (ABT-538) in human liver microsomes. J Pharmacol Exp Ther 1996;277:423–31.

[19] Li Y, Pasunooti KK, Li RJ, Liu W, Head SA, Shi WQ, Liu JO. Novel tetrazole-containing analogues of itraconazole as potent antiangiogenic agents with reduced cytochrome P450 3A4 inhibition. J Med Chem 2018;61:11158–68. doi:10.1021/acs.jmedchem.8b01252.

[20] Er-Rajy M, El Fadili M, Imtara H, Saeed A, Ur Rehman A, Zarougui S, Abdullah SA, Alahdab A, Parvez MK, Elhallaoui M. 3D-QSAR studies, molecular docking, molecular dynamic simulation, and ADMET proprieties of novel pteridinone derivatives as PLK1 inhibitors for the treatment of prostate cancer. Life 2023;13:127 (Basel). doi:10.3390/life13010127.

[21] Zarougui S, Er-rajy M, Faris A, Imtara H, El fadili M, Al kamaly O, Zuhair Alshawwa S, Nasr FA, Aloui M, Elhallaoui M. QSAR, DFT studies, docking molecular and simulation dynamic molecular of 2-styrylquinoline derivatives through their anticancer activity. J Saudi Chem Soc 2023;27:101728. doi:10.1016/j.jscs.2023.101728.

[22] Lenda F, Guenoun F, Tazi B, Ben larbi N, Allouchi H, Martinez J, Lamaty F. Synthesis of new tetrazole-substituted pyroaminoadipic and pipecolic acid derivatives. Eur J Org Chem 2005;2005:326–33. doi:10.1002/ejoc.200400328.

[23] Er-rajy M, Fadili ME, Mujwar S, Lenda FZ, Zarougui S, Elhallaoui M. QSAR, molecular docking, and molecular dynamics simulation–based design of novel anti-cancer drugs targeting thioredoxin reductase enzyme. Struct Chem 2023;34:1527–43. doi:10.1007/s11224-022-02111-x.

[24] Wishart DS, Knox C, Guo AC, Shrivastava S, Hassanali M, Stothard P, Chang Z, Woolsey J. DrugBank: A comprehensive resource for in silico drug discovery and exploration. Nucleic Acids Res 2005;34:D668. doi:10.1093/nar/gkj067.

[25] Trott O, Olson AJ. AutoDock Vina: Improving the speed and accuracy of docking with a new scoring function, efficient optimization and multithreading. J Comput Chem 2010;31:455. doi:10.1002/jcc.21334.

[26] Seeliger D, de Groot BL. Ligand docking and binding site analysis with PyMOL and Autodock/Vina. J Comput Aided Mol Des 2010;24:417–22. doi:10.1007/s10822-010-9352-6.

[27] Clark M, Cramer RD III, Van Opdenbosch N. Validation of the general purpose tripos 5.2 force field. J Comput Chem 1989;10:982–1012. doi:10.1002/jcc.540100804.

[28] Matin MM, Uzzaman M, Chowdhury SA, Bhuiyan MMH. *In vitro* antimicrobial, physicochemical, pharmacokinetics and molecular docking studies of benzoyl uridine esters against SARS-CoV-2 main protease. J Biomol Struct Dyn 2022;40:3668–80. doi:10.1080/07391102.2020.1850358.

[29] Matin MM, Chakraborty P, Alam MS, Islam MM, Hanee U. Novel mannopyranoside esters as sterol 14α-demethylase inhibitors: Synthesis, PASS predication, molecular docking, and pharmacokinetic studies. Carbohydr Res 2020;496:108130. doi:10.1016/j.carres.2020.108130.

[30] Matin MM, Bhattacharjee SC, Chakraborty P, Alam MS. Synthesis, PASS predication, *in vitro* antimicrobial evaluation and pharmacokinetic study of novel n-octyl glucopyranoside esters. Carbohydr Res 2019;485:107812. doi:10.1016/j.carres.2019.107812.

[31] Er-Rajy M, El Fadili M, Mujwar S, Zarougui S, Elhallaoui M. Design of novel anti-cancer drugs targeting TRKs inhibitors based 3D QSAR, molecular docking and molecular dynamics simulation. J Biomol Struct Dyn 2023;41:11657–70. doi:10.1080/07391102.2023.2170471.

[32] Daina A, Michielin O, Zoete V. SwissADME: A free web tool to evaluate pharmacokinetics, drug-likeness and medicinal chemistry friendliness of small molecules. Sci Rep 2017;7:42717. doi:10.1038/srep42717.

[33] Abdelrheem DA, Rahman AA, Elsayed KNM, Abd El-Mageed HR, Mohamed HS, Ahmed SA. Isolation, characterization, *in vitro* anticancer activity, dft calculations, molecular docking, bioactivity score, drug-likeness and admet studies of eight phytoconstituents from brown alga *sargassum platycarpum*. J Mol Struct 2021;1225:129245. doi:10.1016/j.molstruc.2020.129245.

[34] Eswaramoorthy R, Hailekiros H, Kedir F, Endale M. In silico molecular docking, DFT analysis and ADMET studies of carbazole alkaloid and coumarins from roots of clausena anisata: A potent inhibitor for quorum sensing. Adv Appl Bioinform Chem 2021;14:13–24. doi:10.2147/AABC.S290912.

[35] Er-rajy M, El fadili M, Mrabti NN, Zarougui S, Elhallaoui M. QSAR, molecular docking, ADMET properties in silico studies for a series of 7-propanamide benzoxaboroles as potent anti-cancer agents. Chin J Anal Chem 2022;50:100163. doi:10.1016/j.cjac.2022.100163.

[36] Oduselu GO, Ajani OO, Ajamma YU, Brors B, Adebiyi E. Homology modelling and molecular docking studies of selected substituted benzo[d]imidazol-1-yl)methyl)benzimidamide scaffolds on plasmodium falciparum adenylosuccinate lyase receptor. Bioinform Biol Insights 2019;13:1177932219865533. doi:10.1177/1177932219865533.

[37] Mujwar S, Tripathi A. Repurposing benzbromarone as antifolate to develop novel antifungal therapy for Candida albicans. J Mol Model 2022;28:193. doi:10.1007/s00894-022-05185-w.